Discover Civil Engineering

Case Study

Seismic performance of deficient reinforced concrete frames in developing countries: a case study in Ramallah city

Mohammad Safi[1] · **Ghada Karaki**[2]

Received: 8 July 2024 / Accepted: 1 October 2024
Published online: 08 October 2024

Abstract
Buildings in developing regions with moderate to high seismicity are more vulnerable to earthquakes. This increased vulnerability is primarily due to the lack of appropriate seismic design guidelines and limited control of construction technologies. This study investigates the design of reinforced concrete (RC) frames in Ramallah city, West Bank, Palestine, identifies their structural deficiencies, and examines the impact of traditional construction technologies on their seismic behavior. The actual response modification factor (R) and ductility ratios were calculated considering local construction skills and construction technologies. Furthermore, a performance-based method was employed to verify whether these frames comply with the anticipated performance outlined by the design standards. Twelve two-dimensional building models were developed and analyzed using nonlinear static analysis to determine the R factors and ductility ratios. The coefficient method (CM) was employed to evaluate the buildings' performance during the considered seismic event and their compliance with the SEI/ASCE 7 (SEI/ASCE7. Minimum Design Loads and Associated Criteria for Buildings and Other Structures (Minimum Design Loads and Associated Criteria for Buildings and Other Structures). 2016) and ACI318 (ACI-318-14: Building Code Requirements for Structural Concrete and Commentary. ACI-318, 2014) design performance objectives. The findings revealed that most frames exhibited ductility factors lower than those assumed in the design process, indicating subpar performance and inadequate seismic design. Structural deficiencies and building height adversely affect performance, resulting in reduced ductility. Furthermore, buildings with stone-concrete or masonry-concrete infills exhibit compromised ductility and plastic strain energy capacity while enhancing strength and stiffness. The study highlighted that most frames failed to meet the life safety performance level required under design seismic events.

Keywords Performance-based assessment · Seismic behavior · Nonductile frames · Reinforced concrete

1 Introduction

Among the most destructive natural hazards, earthquakes cause extensive damage to structures and infrastructure, with significant economic and social consequences. Consequently, earthquake engineering has emerged as a critical interdisciplinary field focused on mitigating these impacts. In recent decades, the concept of performance-based seismic assessment has been initiated due to major developments in structural seismic analysis and design. Traditionally, seismic design codes provide enforceable criteria that can achieve a minimum level of safety and acceptable performance of

✉ Mohammad Safi, msafi@vols.utk.edu; Ghada Karaki, ghada.karaki@uwe.ac.uk | [1]Department of Civil and Environmental Engineering, University of Tennessee, 325 John D. Tickle Building, Knoxville, TN 37996, USA. [2]School of Engineering, College of Arts, Technology, and Environment, University of the West of England, Bristol, UK.

buildings during an earthquake by specifying a minimum requirement for strength, stiffness, ductility, material properties, and element detailing and configuration. Based on this, the provisions of seismic design codes imply a minimum level of performance. However, the performance of structures not designed or explicitly constructed according to seismic design codes is often not identified by conventional standards or needs assessment.

Many researchers have investigated the global performance of building systems through the use of a response modification factor (R). The response modification factor considers the inelastic deformations formed in buildings due to seismic action and represents the system's capability to dissipate energy as inelastic deformations. The response modification factor (R) for the seismic design of structures was first defined by [3, 4]. Then, the proposals from Newmark and Hall [5] were implemented in both UBC [6] and FEMA [7]. The National Earthquake Hazards Reduction Program [8] proposed the R coefficient to explain the ductility, overstrength, and energy dissipation of structural systems. The response modification factor (R) represents the ductility and seismic performance of a structure used for calculating seismic loads (NEHRP 2001). Researchers have adopted this approach to experimentally and numerically investigate the performance of structural systems. Zafar [9] evaluated the response modification factor R for Pakistan's reinforced concrete moment resisting frames. The calculated R-factors were found to be smaller than those stated in the U.S. seismic codes (SEI/ASCE7-05), indicating a lower seismic performance of structures in Pakistan. Mondal et al. [10] investigated the actual values of response modification factors for realistic reinforced concrete buildings designed and detailed according to Indian standards. These calculated factors were compared with the values suggested in the national design code. The authors concluded that the recommended values of R in the Indian standards are higher than the actual values of R, which is considered unsafe. Chaulagain et al. [11] investigated the actual response modification factor R for irregular RC buildings in Kathmandu Valley, Nepal, through nonlinear static pushover analysis. The authors found that the computed R-factor is less than the recommended value in Indian Standard [12]. Kim and Choi [13] evaluated the response modification factor for both special and ordinary concentrically braced frames. The results showed that the response modification factors are smaller than those recommended by the design codes, indicating an unconservative design. More recent literature [14–18] investigated the actual response modification factor R and recommended different R values.

Furthermore, other studies have examined the effect of structural element ductility on the global performance of structures, such as beam-column joint behavior, inadequate shear capacity, and reinforcing bar–concrete bond-slip effects on beam-column joint behavior. The absence of shear reinforcement leads to significant shear deformation in the joint area, restricting the flexural capacities of the beams and columns joining, resulting in decreased [19–22]. The authors confirmed that RC structures with deficient beam-column joints are vulnerable, especially under severe earthquakes, and additional transverse reinforcement helps decrease the development of shear cracks in the joint area. Lin [23] studied the effects of insufficient lap splices in deficient reinforced concrete frames on system performance. The authors concluded that a 25% deficient lap splice length in laboratory tests does not affect the global response of the structures. Kumbasaroglu [24] included that Anchoring bars in an RC building with infilled walls enhance its seismic performance.

Research has also examined the effect of infills on the seismic performance of buildings. Pandit and Chaulagain [25] studied the effect of masonry infill walls on the response modification factor of existing RC buildings. The inclusion of infills decreased the structure period by 40–60%. Infilling increased the base shear resistance of the structure from 1.2 to 2.2 and reduced the displacement ductility factor by 35–45%. Patel and Vasanwala [26] assessed the response modification factor of unreinforced masonry-infilled RC buildings. The study showed that including infill walls decreased the ductility factor while the overstrength factor increased. Ko et al. [27] examined the seismic behavior of a low-rise RC moment-resisting frame with masonry infill walls. The study results indicated that including masonry infill walls increases the structure's global stiffness and decreases its natural period and ductility. Kumbasaroglu [24], Kumbasaroğlu and Budak [28] also confirm that infilled walls increase stiffness and reduce the ductility of RC buildings.

Despite extensive research on the seismic performance of frame structures, a limited number of studies have investigated and assessed the seismic performance of buildings in Palestine, given that the area has suffered from earthquakes sourced mainly from the Dead Sea fault. Historical records show that major earthquakes have caused severe damage to buildings and losses in human life [29]. According to Shapira [30] and Abou Karaki [31], most of the recorded earthquakes have magnitudes ranging between 1.0 and 6.5 on the local magnitude (ML) scale. Al-Dabbeek and El-Kelani [32] assessed the seismic vulnerability of RC buildings on Palestinian camps. They found that severe structural and nonstructural damage will occur in many buildings due to anticipated moderate or strong earthquakes. Furthermore, Al-Dabbeek [33] studied the expected seismic performance of buildings in Palestine and reported that one-third of the investigated buildings are likely to suffer heavy damage, whereas approximately 40% of the buildings may suffer moderate damage. Salahat [34] performed a seismic performance-based assessment and retrofitting of a typical reinforced concrete building in Palestine. The results showed that the performance assessment of existing buildings in Palestine cannot meet the required performance level (IO) under earthquake loading. The seismic performance of reinforced concrete frames in Palestinian cities has not been reported in the literature considering the influence of traditional construction practices, local seismic behavior, and design deficiencies (mainly in the detailing of reinforcement). Therefore, this paper aims to investigate the effectiveness of seismic design for RC buildings in Ramallah, focusing on buildings assumed to be designed for seismic loads following SEI/ASCE7 [1] and ACI318 [2]. In regions without national standards, particularly in the Middle East, international standards such as SEI/ASCE7 [1] and ACI318 [2] are often adopted for concrete structures [35, 36]. Although these standards are widely recognized and applied, there is a growing need to evaluate their compatibility with local building technologies and construction practices. This study addresses this gap by examining the performance of reinforced concrete frames within the context of local construction technologies in Ramallah. Since the construction methods across the region exhibit similarities, this analysis provides valuable insights into the applicability of international seismic standards. In this investigation, the actual response modification factor (R) and ductility ratios were calculated considering local construction skills and construction technologies. A performance-based method was employed to verify whether these frames comply with the anticipated responses outlined by the design standards.

2 Selection of frame structures

2.1 Data collection

This section maps the typical structural systems and considers deficiencies through semi-structured interviews held with highly skilled/active engineers, contractors, and construction managers. The interviews showed that reinforced concrete frame buildings are the most common building category in major Palestinian cities, especially Ramallah. Reinforced concrete shear walls are often used around stairwells and elevators; their poor positioning prevents the lateral resisting system from being categorized as a shear-wall system or dual system. Grigoratos et al. [37] reached a similar conclusion regarding similar structural systems in the region, and the study was used to control and verify the output of the data collection. The findings indicated that most buildings have four to six floors or six to nine floors. The typical inter-story height in these buildings is 3.0 m. However, for mixed-use buildings, i.e., commercial/residential buildings, the ground floor has a height of 6.0 m, and the remaining floors have a height of 3.0 m. The bays range from 3.0 m to 6.0 m long, with a typical span of 4 m. The surveyed buildings had regular floor plan layouts.

Furthermore, most RC buildings have external stone-concrete infill walls ranging from 25 to 35 cm thick [38]. These infill walls consist of stone, plain concrete, insulation boards, and concrete masonry, as shown in Fig. 1. Due to this construction method, there is an interaction between the infills and other structural components, which adds to the lateral stiffness of the frame and causes an increase in the global stiffness and strength of the frame system and a decrease in ductility. The interviewed experts were asked to identify the common deficiencies noticed at construction sites. They reported that most buildings have a structural deficiency in the beam-column joint area, i.e., the discontinuity of the column's transverse reinforcement within the joint. Inadequate development lengths in the beams, columns, and beam-column joints were also recognized. The interviewed engineers also remarked that the shear reinforcement and stirrup spacing were insufficient for new and existing buildings.

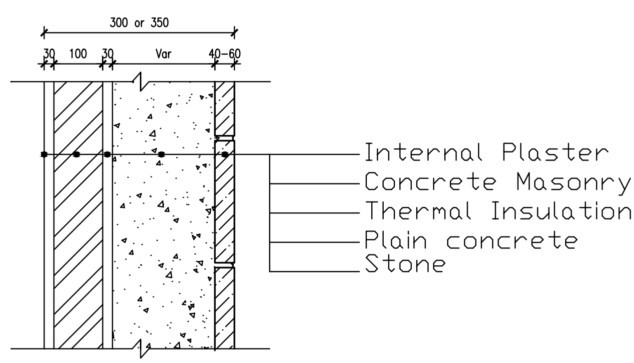

Fig. 1 Typical cross-section of the stone-concrete infill panel, dimension in mm (plain concrete and stone thicknesses are varied since the total thickness of infill wall is not a standard thickness)

2.2 Frame structures

To investigate the seismic performance of deficient reinforced concrete frames and informed by expert opinion, twelve 2D RC-moment resisting frames (MRFs) were chosen as typical RC frames built in Ramallah. Two prototype RC-MRFs had three bay-six stories (3B6S): one bare ductile frame and one bare nonductile frame. In a nonductile frame, the following structural deficiencies were modeled: no transverse reinforcement in the beam−column joint area, inadequate development length, and inadequate shear reinforcement in the beams and columns. The four prototypes of RC-MRFs were three bay-six stories (3B6S) with infill walls (stone-concrete and concrete masonry). Furthermore, two prototype RC-MRFs were three bay-nine stories (3B9S): bare ductile and nonductile frames. The other four 3B9S frames had infill walls. The geometrical data of the selected prototypes are summarized in Table 1.

These prototype RC-MRFs are assumed to be designed according to SEI/ASCE7 [1] and ACI-318 [2] as intermediate moment-resisting frames (for which the R factor equals 5). The cross-sections and steel reinforcements of the typical beams and columns, as shown in Fig. 2 were designed using a typical concrete cylinder compressive strength of 28 MPa. The steel reinforcement used has a yield strength of 420 MPa and a modulus of elasticity of 200,000 MPa. Notably, each prototype is assigned dead and live loads (gravity loads) according to both SEI/ASCE7[1]. The superimposed dead load is 4.5 kN/m^2, the live load is 3 kN/m^2, and the weight of the infill walls is 20 kN/m with a thickness of 0.3 m as a typical value.

3 Methods

3.1 Response modification factor using nonlinear static analysis

The response modification factor R was calculated based on the method proposed by ATC [39], which considers factors that account for the overall strength, ductility, and redundancy of a structure. These factors were evaluated by running a nonlinear static pushover analysis and developing the capacity curve for each building category, as shown in Fig. 3, which compares ideal and actual inelastic behavior of a structure under lateral loading. The "Idealized Bilinear Envelope" represents a simplified response of how the structure should ideally behave, while the "Actual Capacity Envelope" shows the real response, including any deviations from the ideal due to material or structural complexities. The response modification factor R was calculated and evaluated based on the pushover analysis results. The factor that accounts for the overstrength (R_s) of the structures was estimated using the maximum base shear (V_0) and the designed base shear (V_d) using Eq. (1). The ductility factor (R_μ) was calculated based on the displacement ductility ratio (μ) using Eqs. (2–4) and depends mainly on the natural period of the structure [5]. In contrast, the redundancy factor (R_r) takes into consideration the reliability of seismic frame systems that use multiple vertical framing lines in each main direction of the building (the redundancy factor (R_r) was taken from Table 2, which is based on ATC [39]).

$$R_s = \frac{V_0}{V_d}. \tag{1}$$

If $0.12 \le$ period (T) ≤ 0.5 s:

Table 1 Selection of model characteristics

Category	Common characteristics	Selected characteristics
Construction material	Reinforced concrete	Reinforced concrete
Structural system	MRFs	MRFs
Number of stories	4–6, 6–9	6 and 9
Number of bays	3–6	3
Plan regularity	Regular	Regular
Plan symmetry	Symmetrical	Symmetrical
Elevation regularity	Regular	Regular
Occupancy	Residential and commercial	Residential and commercial
Floor area (m^2)	100–500	100–500

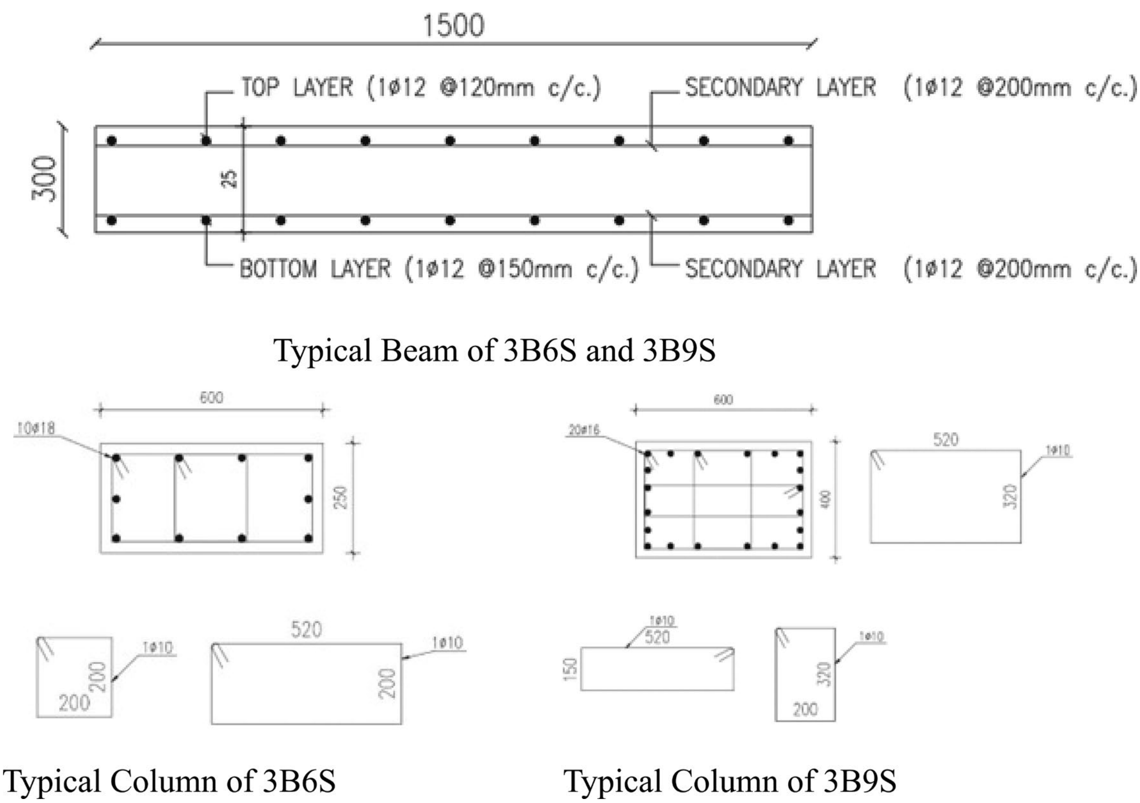

Fig. 2 Cross-sections and steel reinforcements of the typical beam and columns, dimensions in mm

Fig. 3 Ideal and actual inelastic response (capacity curve) [41]

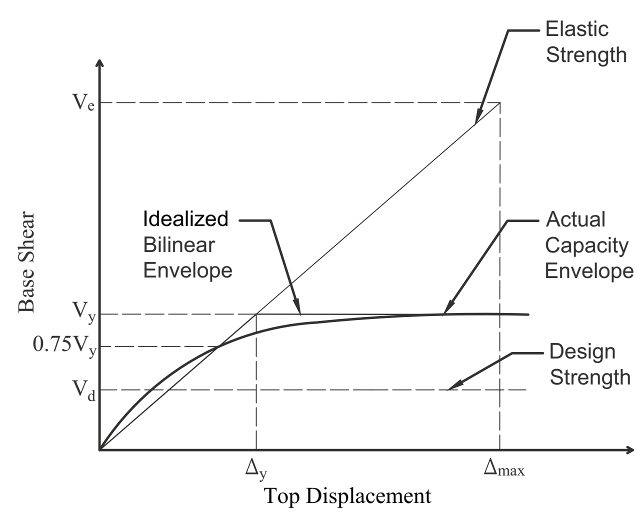

Table 2 Redundancy factor based on ATC [39]

Lines of vertical seismic framing	Redundancy factor
2	0.71
3	0.86
4 (or more)	1.00

$$R_u = (2 * u - 1)^{0.5}, u = \frac{\Delta_{max}}{\Delta_y} (both\ parameters\ illistrated\ in\ Fig. 3). \tag{2}$$

If 0.5 < T < 1.0 s:

$$R_u = (2 * u - 1)^{0.5} + 2(T - 0.5) * \left(u - (2 * u - 1)^{0.5}\right). \tag{3}$$

If 1.0 s ≤ T:

$$R_u = u. \tag{4}$$

3.2 Seismic performance assessment: coefficient method

Based on the previous section, the behavior of the structural systems was further examined by carrying out a performance-based evaluation of the buildings. The performance-based method relates a seismic event and a structural ability to resist that event. The assessment was performed by determining the performance of a frame system and comparing it with the required performance objectives. Furthermore, the structure's response should meet the selected acceptance criteria adopted by SEI/ASCE-41 [40]. According to the SEI/ASCE-41 [40] standard, the principles of the seismic performance-based method (coefficient method) can be applied to determine the performance point for each frame system. The displacement coefficient method (CM) is widely used to estimate the target displacement in a nonlinear static pushover procedure (NSP). This method was adopted in accordance with the SEI/ASCE-41 [40] standard. The coefficient method (CM) utilizes a displacement modification procedure to calculate the target displacement for a linearly elastic single-degree-of-freedom system (SDOF) using several coefficients, as shown in Eq. (5), where coefficient C_0 relates the elastic response of an SDF system to the elastic displacement of the MDF building at the control node taken as the first mode participation factor, $C_1, andC_2$ accounts for various site classes, S_a is the response spectrum acceleration at the effective fundamental vibration period and damping ratio of the building under consideration, g is the acceleration due to gravity, and T_e is the effective fundamental period of the building in the direction under consideration computed by modifying the fundamental vibration period from elastic dynamic analysis. According to the interviews, most of the Palestinian buildings are commercial-residential. Therefore, the target performance level is Life Safety (LS), which is the performance requirement used in most seismic design codes. SEI/ASCE-41 [40] defines the life safety performance level as 0.75 times the deformation at point E, as shown in Fig. 4.

$$\delta_t = C_0 C_1 C_2 S_a \left(\frac{T_e^2}{4\pi^2}\right) g. \tag{5}$$

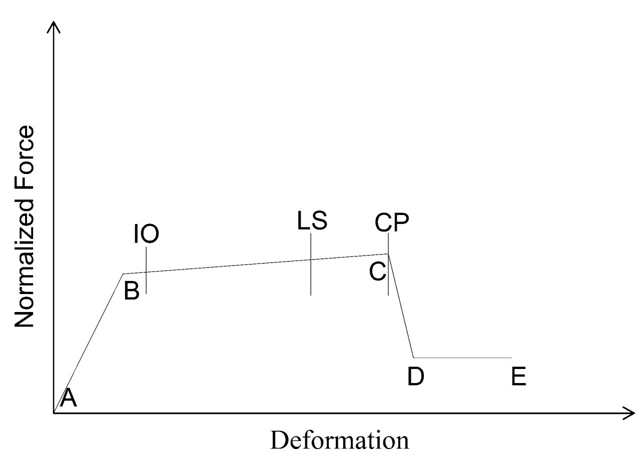

Fig. 4 Illustration of the acceptance criterion [40]

4 Numerical modeling

4.1 Material models

Numerical models for the examined structural systems were developed using an open-source finite element program to investigate the performance of the buildings considering the identified deficiencies. The structural elements, beams, columns, and shear walls are defined as nonlinear elements with fiber sections to model the frame elements (lumped plasticity models with predefined plastic hinges were used to represent the nonlinear behavior of the frame elements). Uniaxial material models predefined in OpenSees are employed to define the constitutive behavior of concrete and steel materials. According to Mazzoni et al. [42], the force–deformation relationship of a section is evaluated through numerical integration of the nonlinear uniaxial material constitutive behavior of the fibers. The force–displacement behavior of the element is obtained by numerical integration of the section force–deformation behavior along the length of the element.

4.1.1 Concrete model

The constitutive material model, which is defined as Concrete02, is used to model confined and unconfined concrete. This model considered the compression and tensile strength of the concrete material [43]. The parameters required to define Concrete02 are depicted in Fig. 5a, which shows the typical stress—strain model proposed for monotonic loading of confined and unconfined concrete. Furthermore, the parameters of the confined concrete were determined based on a study by Mander et al. [44] to consider confinement due to transverse reinforcement.

4.1.2 Steel reinforcement model

The steel reinforcement is modeled using the Steel02 constitutive model. The input parameters required to define the Steel02 model are the yield strength (F_y), initial elastic tangent (E), and strain hardening ratio (b), which is defined as the ratio between the post-yield tangent and initial elastic tangent, and three constants (R0, cR1, and cR2) to control the transition from the elastic to the plastic range. Figure 5b shows the material law with the main input variables [42].

4.1.3 The beam—column joint model

The beam-column joint was modeled according to Lowes and Altoontash [45]. The bonding-slip response of the beam-column longitudinal reinforcement was modeled as eight zero-length translational springs. The uniaxial material barrier

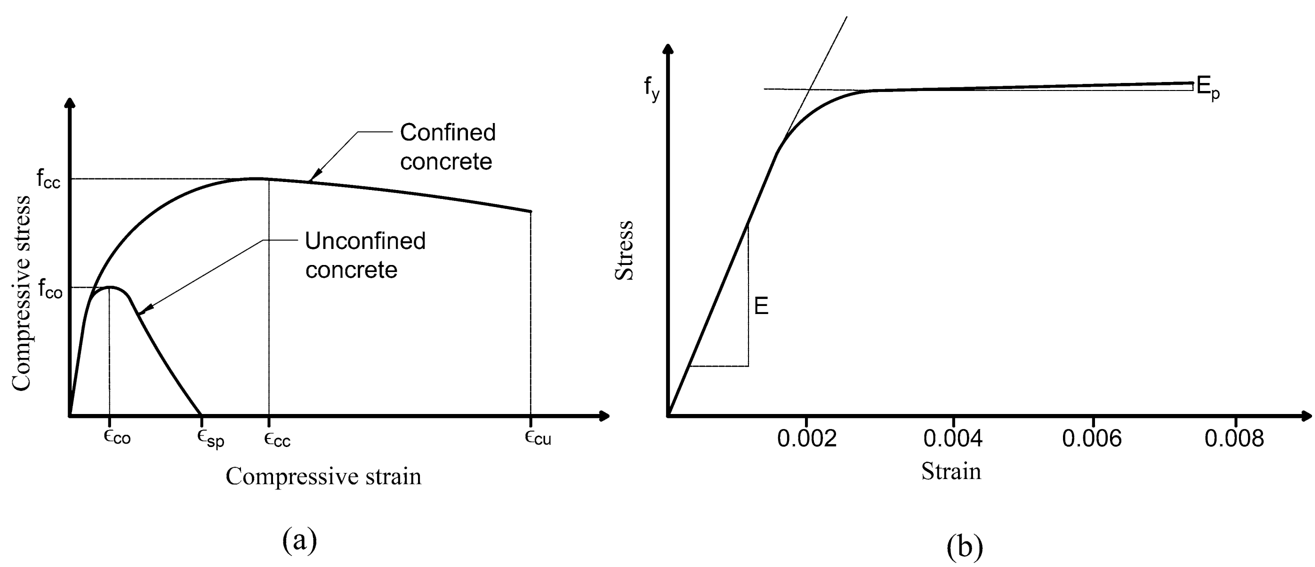

Fig. 5 **a** Stress—strain model proposed for monotonic loading of confined and unconfined concrete [44] and (**b**) stress—strain relationship assumed for steel reinforcement [42]

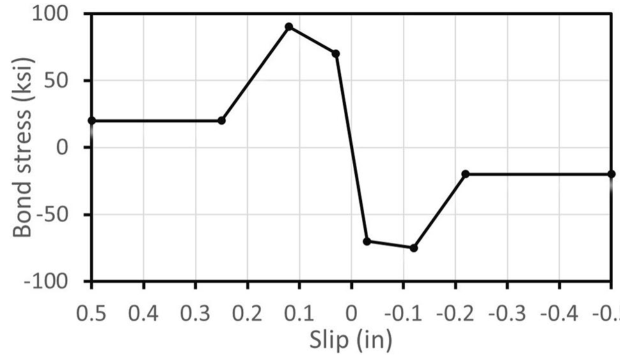

Fig. 6 Envelope for Hysteretic Bar Slip Versus Slip Response [45, 46]

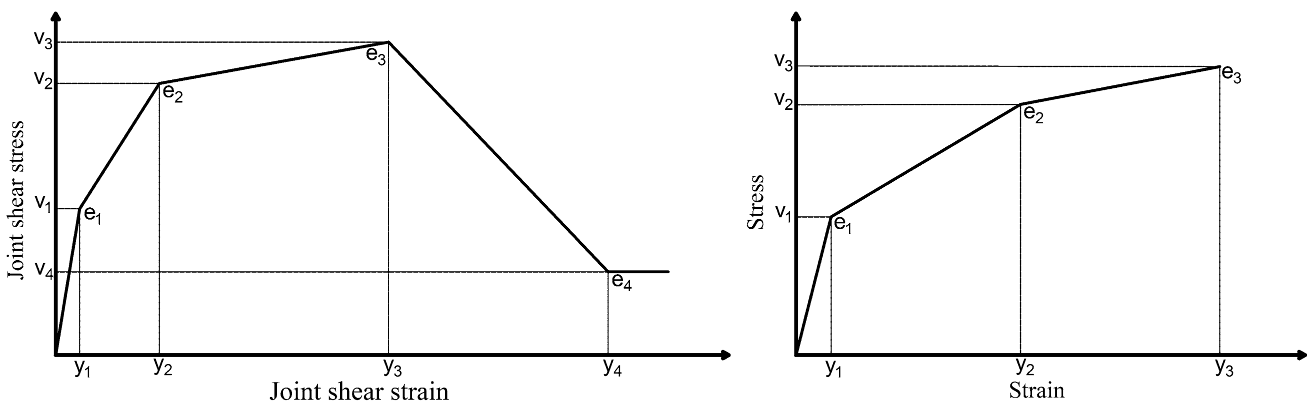

(a) (b)

Fig. 7 **a** Envelope of the joint shear stress–strain relationship [49] and (**b**) the backbone curve for joints without transverse reinforcement [47]

slip constitutive model was used to define the bonding-slip response, calibrated by Lowes and Altoontash [45]. Figure 6 shows the relationship between the bond stress and the slip of the steel bar within the joint [45, 46]. The four zero-length shear springs simulate the interface-shear deformations and are defined as elastic uniaxial materials. The zero-length rotational spring represents the joint's shear deformations with uniaxial material pinching to determine the pinched load–deformation response. The input parameters of the pinching material are the envelope stresses and strains, which define the backbone curve for the shear panel, as shown in Fig. 7a. The first two points of the backbone curve were taken from Anderson et al. [47], which was developed for beam-column joints without transverse reinforcement. The third point was determined based on Eqs. (6) and (7) by Kim et al. [48]. Where α_1 describes the in-plane geometry: 1.0 for interior connections, 0.7 for exterior connections and 0.4 for knee connections; β_1 is a parameter for describing out-of-plane geometry: 1.0 for subassemblies with zero or one transverse beam and 1.18 for subassemblies with two transverse beams; η_1 describes joint eccentricity (equals 1.0 with no joint eccentricity); $JI = (p_j x f_{yj})/f_c\prime$ is the joint transverse reinforcement index in which p_j is the volumetric joint transverse reinforcement ratio, f_{yj} is the yield stress of joint transverse reinforcement, and $f_c\prime$ is the concrete compressive strength; $BI = (p_b x f_{yb})/f_c\prime$ in which p_b is the beam reinforcement ratio and f_{yb} is the yield stress of beam reinforcement; $\alpha_{\gamma 1} = JPRU^{2.1}$ in which the value of *JPRU* relies on the steel reinforcement ratio; $\beta_{\gamma 1}$ describing out-of-plane geometry (1.0 for subassemblies with zero or one transverse beam and 1.4 for subassemblies with two transverse beams); and $\eta_{\gamma 1}$ describes joint eccentricity (equals 1.0 with no joint eccentricity). The fourth point represents the residual strength equal to 20% of the maximum shear strength. In the case of beam-column joints without transverse reinforcement, the first two points were the same. The maximum shear strength at the third point was calculated by extrapolating the second and third points, knowing the strain at the maximum shear strength (third point) and the slope of the segment (e2–e3). Figure 7b shows the backbone curve for joints without transverse reinforcement.

$$v_j(MPa) = 1.07\alpha_1 * \beta_1 * \eta_1 * (JI)^{0.15} * (BI)^{0.3} * \left(f_c\prime\right)^{0.75}, \quad (6)$$

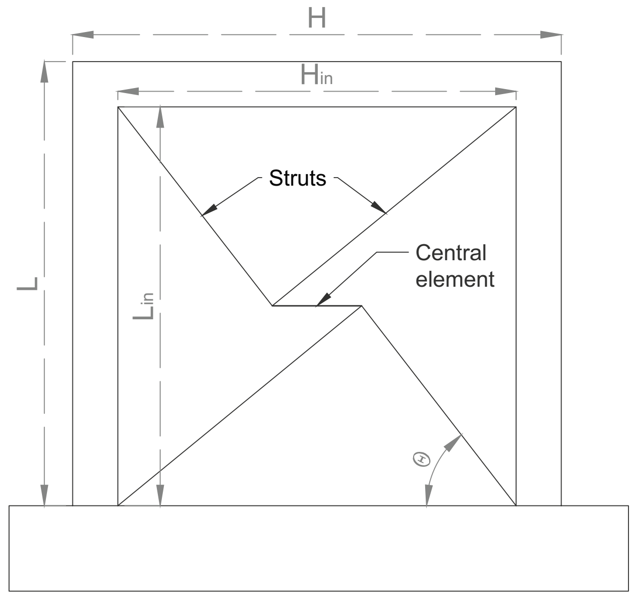

Fig. 8 Macro model for simulating an infill panel [50]

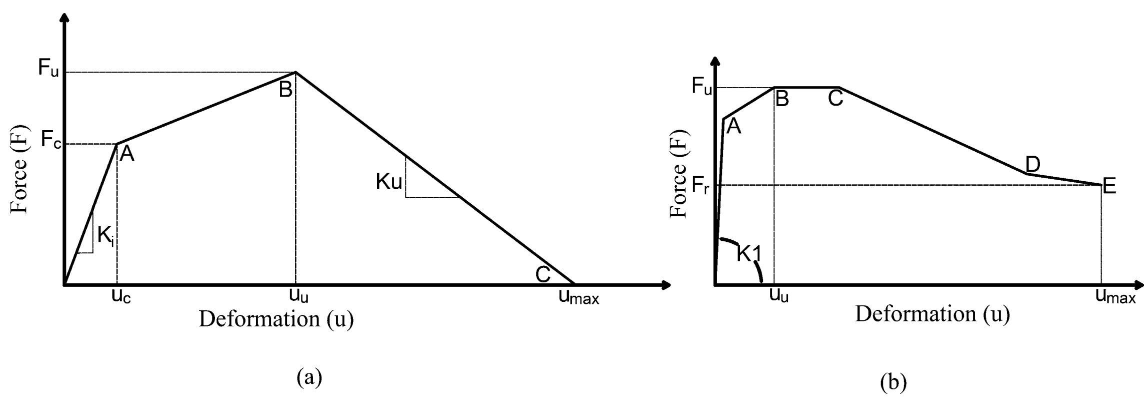

Fig. 9 **a** Force–deformation relationship for masonry infill walls [38] and **b** force–deformation relationship for stone–concrete infill walls [38]

$$\gamma(rad) = \alpha_{\gamma 1} * \beta_{\gamma 1} * \eta_{\gamma 1} * (JI)^{0.10} * BI * \left(\frac{v_i}{f\ {}_c{}'}\right)^{1.75}. \tag{7}$$

4.1.4 Infill walls model

According to Rodrigues [50], infill walls are modeled using an equivalent bidiagonal-strut model. This model accurately represents the global response and energy dissipation mechanisms of structures with infill walls. The typical bidiagonal strut model represents infill panels as four support strut elements with rigid behavior. The central strut element considers the nonlinear behavior of the infill wall, as shown in Fig. 8. Using OpenSees, the four diagonal elements were modeled as elastic beam columns and nonlinear beam columns for the central elements. The nonlinear monotonic behavior of the central element was idealized as a pinching material. The parameters required to define the concrete masonry infill wall constitutive model can be obtained following the recommendations of different authors and international codes. According to Mainstone [51], the thickness of the strut model (*tw*) is the same as that of the infill wall, the width of the strut model can be evaluated using Eqs. (8) and (9), and the initial lateral stiffness K_{in} is based on Eq. (10). The strut element carries only compression, and its constitutive model force–deformation envelope curve is shown in Fig. 9a. Envelope values were developed based on the equations and the recommended model values from Mainstone [51] and Dolšek and Fajfar [52]. The maximum strength of the infill walls was determined using simplified Eq. (11) [53].

Al-Nimry [54], Al-Nimry [55], Al-Nimry [56] investigated the lateral response of RC frames with stone-concrete infill walls and concluded that the stone-concrete infill panels could be modeled using two nonlinear link elements. Each element is assigned a multilinear plastic property with only nonlinear behavior in the axial direction. The constitutive model of the stone-concrete infill panel is shown in Fig. 9b. According to [54–56], the initial axial stiffness is estimated based on the equation Fajfar et al. [57], as given in Eq. (12). The modulus of elasticity of the infill panel (*Ep*) was assumed to be 14.0 GPa, and the effective width of the equivalent strut can be taken as one-tenth the length of the equivalent strut. In Eqs. (8) through (12), the parameters used include H, which represents the height of the infill panel, L is the length of the equivalent strut, E_w refers to the modulus of elasticity of the wall material, the effective width of the equivalent strut is represented by W_{eff}, θ is the angle of inclination of the strut, r is the radius of gyration of the infill wall, f_{tp} denotes the tensile strength of the panel material, F_{max} represents the maximum strength of the infill panel, L_{in} represents the length of the infill wall, E_c is the modulus of elasticity of the concrete, I_c is the moment of inertia of the concrete section, and H_{in} is the height of the infill wall.

$$W_{eff} = 0.175\left(\lambda_h * H\right)^{-0.4} * \left(H^2 + L^2\right)^{0.5}. \tag{8}$$

$$\lambda_h = \left(\frac{E_w * t_w * \sin(2 * \theta)}{4 * E_c * I_c * H_{in}}\right)^{0.25}. \tag{9}$$

$$K_{in} = \left(E_w * W_{eff} * \frac{t_w}{\left(L^2 + H^2\right)^{0.5}}\right) * (\cos\theta)^2 \tag{10}$$

$$F_{max} = F_u = 0.818 * \frac{L_{in} * t_w * f_{tp}}{C_1} * \left(1 + \left(C_1^2 + 1\right)^{0.5}\right), C1 = 1.925 * \left(\frac{L_{in}}{H_{in}}\right), \tag{11}$$

$$K_{in} = \left(E_w * W_{eff} * \frac{t_w}{r}\right). \tag{12}$$

4.2 Model verification

The numerical analysis results were validated against experimental data from the open literature. The nonlinear analysis data available for the RC frame obtained by Vecchio and Emara [58] were utilized to verify the developed model. The frame spans 3500 mm c/c, and the first and second story heights are 2200 mm c/c. The beams and columns are 400 mm deep and 300 mm wide. The material properties included the following: the compressive strength of the concrete was 30 MPa; the steel properties included a yield strength of 418 MPa, an ultimate tensile stress of 596 MPa, a modulus of elasticity of 192,500 MPa, and a strain hardening modulus of 3100 MPa; and the shear reinforcement had a yield strength of 454 MPa and an ultimate stress of 640 MPa. An axial load of 700 kN was applied to each column from the top end to activate the p-delta effect [58]. Figure 10a, b show good agreement between the experimental and numerical analysis results.

The data available from Cavaleri, et al. [59] were used to verify the infill wall model. The frame spans 1800 mm c/c, and the story height is 1800 mm c/c. The beams are 400 mm deep and 200 mm wide. The columns are 200 mm deep and 200 mm wide. The material properties included the following: the compressive strength of the concrete was 30 MPa, the steel properties were as follows: the yield strength was 434 MPa, and the modulus of elasticity was 190,000 MPa. A 200 kN axial load was applied to each column from the top end. Material properties of the infills: The compressive strength of the infill is 3 MPa, and the elasticity modulus is 7350 MPa. The two frame systems were modeled using beam and column elements without the beam—column joint model. Both the beams and columns were modeled as force beam—column elements. The infills were modeled according to Rodrigues [50] with the corresponding behavior of the masonry infill wall. The results of both models were compared using the capacity curves provided by Rodrigues [50] and Cavaleri et al. [59], as shown in Fig. 10c, d, respectively. A good correlation is also observed between the experimental and numerical results. The model was used to examine the impact of structural deficiencies in construction practices on the capacity curve of the frame system. Inadequate stirrup spacing in both the beams and columns, inadequate joint detailing, and

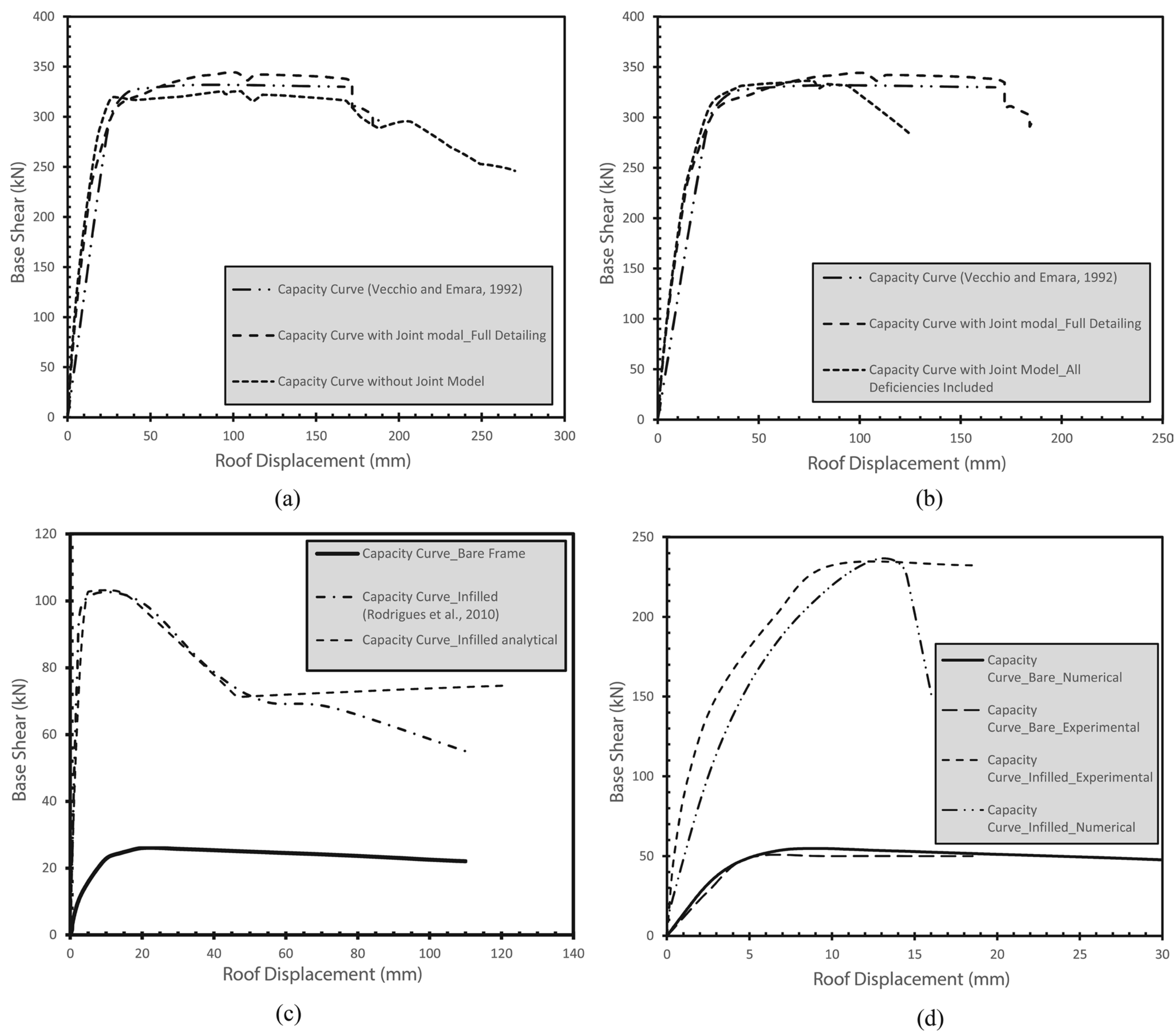

Fig. 10 **a** Verification of the pushover analysis model without a joint model; **b** capacity curve including the deficiencies of the model; **c** verification of the pushover analysis model from [50]; and (**d**) verification of the pushover analysis model from [59]

short anchorage of longitudinal bars in the joint were considered. The analysis results presented in Fig. 10b show that including these deficiencies dramatically decreases the ductility of the frame.

5 Analysis and assessment of seismic performance

5.1 RC MRF prototypes and their analysis

As described earlier, the selected frames show the effects of structural deficiencies, infill walls (stone-concrete and masonry concrete), and soft story mechanisms (ground level without infills) on the response modification factors and ductility ratios of buildings. Figure 11 shows a typical prototype model for 3B6S and 3B9S. To perform nonlinear analysis, modal analysis was first conducted on each prototype model to determine the fundamental elastic period of vibration. The period was used to calculate the displacement ductility ratio (μ), which is the most critical factor in R-factor evaluation. The results from the modal analysis for each prototype model are summarized in Table 3. Notably, frames with infills (either stone-concrete or masonry-concrete) consistently exhibit shorter fundamental periods than

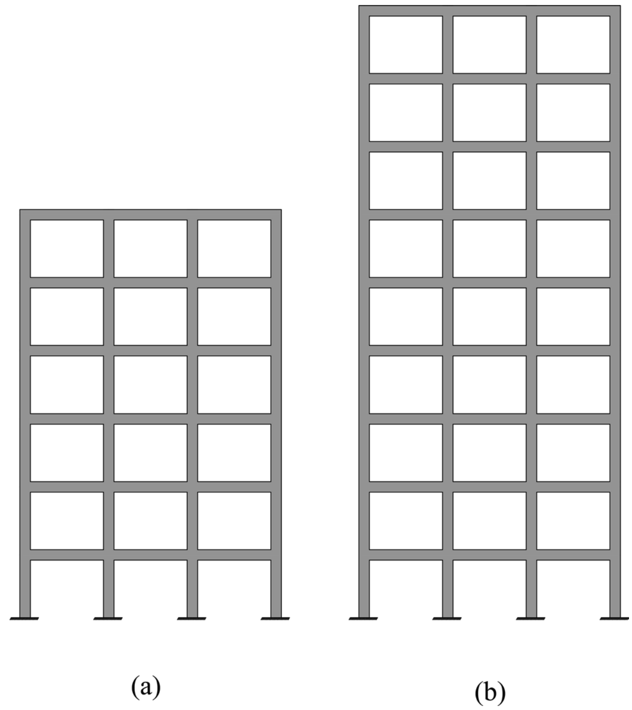

Fig. 11 **a** Elevation of three bay-six stories (3B6S). **b** Elevation of three bay-nine stories (3B9S)

Table 3 Fundamental period for each prototype model

	Building system	Fundamental period T_i (s)
(1)	3B6S MRFs-bare frame	0.78
(2)	3B6S MRFs-bare frame with structural deficiencies	0.75
(3)	3B6S MRFs-stone-concrete infilled frame	0.49
(4)	3B6S MRFs-stone-concrete infilled frame without ground infills	0.49
(5)	3B6S MRFs-masonry-concrete infilled frame	0.45
(6)	3B6S MRFs-masonry-concrete infilled frame without ground infills	0.45
(7)	3B9S MRFs-bare frame	1.07
(8)	3B9S MRFs-bare frame with structural deficiencies	1.01
(9)	3B9S MRFs-stone-concrete infilled frame	0.70
(10)	3B9S MRFs-stone-concrete infilled frame without ground infills	0.70
(11)	3B9S MRFs-masonry-concrete infilled frame	0.67
(12)	3B9S MRFs-masonry-concrete infilled frame without ground infills	0.67

their bare frame counterparts, indicating stiffer systems due to the additional infill material. The presence or absence of structural deficiencies slightly alters the fundamental period, typically reducing it, which may indicate changes in dynamic properties due to compromised structural integrity. The effect of infills appears significant, consistently decreasing the fundamental period across different frame configurations. A nonlinear static pushover analysis was performed for each prototype model, and the results are shown in Figs. 12a–f and 13a–f. The results of the pushover curves of 3B6S and 3B9S Moment-Resisting Frames (MRFs) show the influence of infills and structural deficiencies on frame performance. Infilled frames, whether masonry-concrete or stone-concrete, exhibit markedly higher base shear capacities compared to bare frames, underscoring the importance of infills in enhancing structural stiffness and strength. Moreover, the presence of structural deficiencies bare frames leads to a noticeable reduction in base shear capacity, highlighting the adverse impact of such deficiencies on structural integrity. Although the differences between frames with and without ground infills are less pronounced, they still contribute to overall structural behavior. Comparatively, 3B9S configurations generally show higher base shear capacities than 3B6S configurations, suggesting variations in design or additional structural elements.

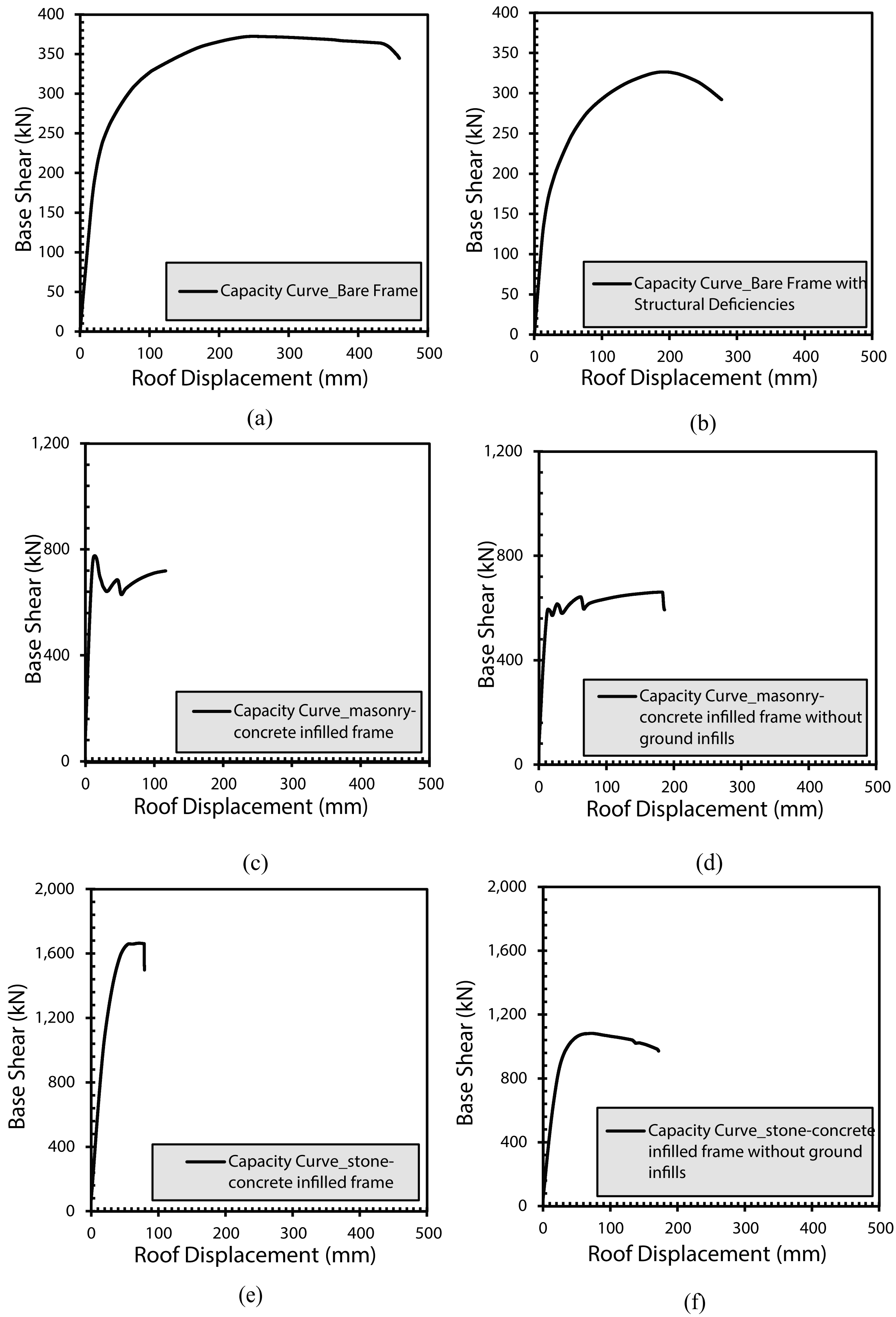

Fig. 12 Pushover curves of the 3B6S MRF (**a**) bare frame; **b** bare frame with structural deficiencies. **c** Masonry-concrete infilled frame; (d) masonry-concrete infilled frame without ground infills; **e** stone-concrete infilled frame; and (**f**) masonry-concrete infilled frame without ground infills

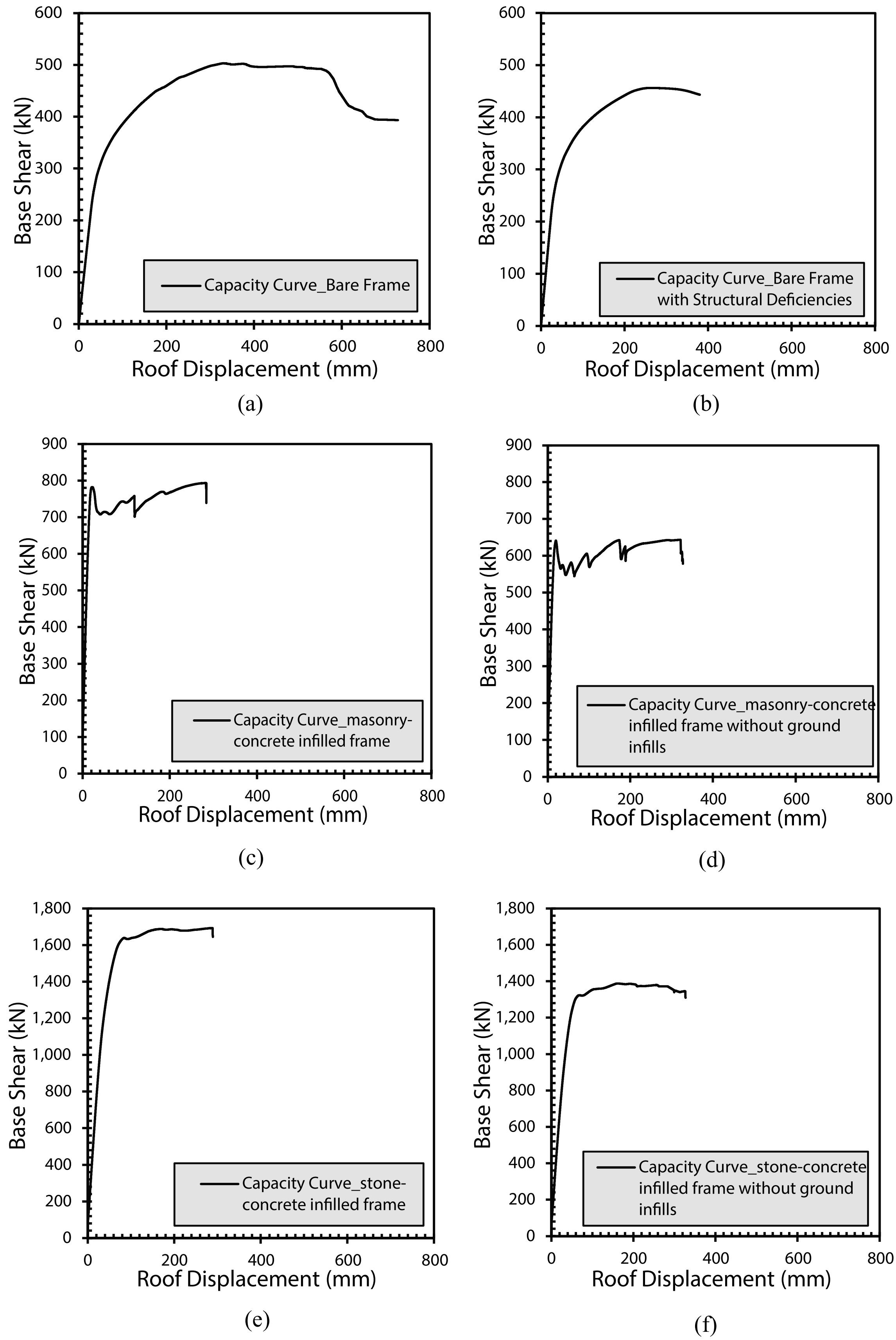

Fig. 13 Pushover curves of the 3B9S MRF (**a**) bare frame; **b** bare frame with structural deficiencies. **c** Masonry-concrete infilled frame; **d** masonry-concrete infilled frame without ground infills; (**e**) stone-concrete infilled frame; and (**f**) masonry-concrete infilled frame without ground infills

Table 4 Records of the calculations of the R-factor

	Building system	Ductility factor (R_{μ})	Over strength factor (R_0)	Redundancy factor (R_r)	Overall R
(1)	3B6S MRFs-bare frame	4.03	1.81	0.86	6.30
(2)	3B6SMRFs-bareframewith structural deficiencies	2.47	1.60	0.86	3.40
(3)	3B6SMRFs-stone-concreteinfilled frame	1.87	–	–	1.87
(4)	3B6SMRFs-stone-concreteinfilled frame without ground infills	3.20	–	–	3.20
(5)	3B6S MRFs-masonry-concrete infilled frame	3.26	–	–	3.26
(6)	3B6S MRFs-masonry-concrete infilled frame without ground infills	4.17	–	–	4.17
(7)	3B9S MRFs-bare frame	4.75	1.51	0.86	6.20
(8)	3B9SMRFs-bareframe with structural deficiencies	2.98	1.37	0.86	3.50
(9)	3B9SMRFs-stone-concreteinfilled frame	2.93	–	–	2.93
(10)	3B9SMRFs-stone-concreteinfilled frame without ground infills	3.67	–	–	3.67
(11)	3B9S MRFs-masonry-concrete infilled frame	–	–	–	–
(12)	3B9S MRFs-Masonry-concrete infilled frame without ground infills	–	–	–	–

Table 5 Comparison between the calculated R and recommended R factors from the adopted seismic codes and standards, and the used R-factor in the analysis

	Building system	Overall R	R (used in the analysis)	R (ASCE 7–16)	R (Europe, EC8)
(1)	3B6S MRFs-bare frame	6.30			
(2)	3B6SMRFs-bareframewith structural deficiencies	3.40			
(3)	3B6SMRFs-stone-concreteinfilled frame	1.87			
(4)	3B6SMRFs-stone-concreteinfilled frame without ground infills	3.20			
(5)	3B6S MRFs-masonry-concrete infilled frame	3.26			
(6)	3B6S MRFs-masonry-concrete infilled frame without ground infills	4.17	5	8	5
(7)	3B9S MRFs-bare frame	6.20			
(8)	3B9SMRFs-bareframewith structural deficiencies	3.50			
(9)	3B9SMRFs-stone-concreteinfilled frame	2.93			
(10)	3B9SMRFs-stone-concreteinfilled frame without ground infills	3.67			
(11)	3B9S MRFs-masonry-concrete infilled frame	–			
(12)	3B9S MRFs-masonry-concrete infilled frame without ground infills	–			

5.2 Evaluation of the ductility ratios and R factors

The ductility and response modification factors for each prototype model are computed based on the previously explained procedure; the calculated values of R are presented in Table 4. Table 4 shows that the bare frames with no deficiencies (3B6S and 3B9S) have ductility factors (R_{μ}) of 4.026 and 4.75 and overstrength factors (R_0) of 1.81 and 1.51, respectively. Compared with the designed R-value of 5 (see Table 5), these frames performed relatively well. However, the bare frames with structural deficiencies (3B6S and 3B9S) have ductility factors (R_{μ}) of 2.47 and 2.98 and overstrength factors (R_0) of 1.6 and 1.37, respectively. These frames exhibit a considerable loss in ductility and the ability to dissipate energy through inelastic behavior. The ductility factor ($R\mu$) of the 3B6S/3B9S masonry-concrete filled frames with/without infill frames ranges from 2 to 4. This variation is due to the rigidity of the infilled frames and the occurrence of the soft story mechanism. The overstrength factor (R_0) was not calculated for the infilled frames because no design criteria anticipate the maximum elastic forces that the infilled frames can carry along with the structural elements. It was not possible to identify the ductility ratios for the stone-infilled frames. Therefore, a performance analysis is conducted for the examined frames. In general, most of the prototype models exhibit a decrease

Table 6 Target displacement and life safety performance level limits

	Building system	Target displacement (mm)	Maximum displacement (mm)
(1)	3B6S MRFs-bare frame	144.5	345.0
(2)	3B6S MRFs-bare frame with structural deficiencies	144.8	207.8
(3)	3B6S MRFs-stone-concrete infilled frame	90.50	59.20
(4)	3B6S MRFs-stone-concrete infilled frame without ground infills	90.90	128.3
(5)	3B6S MRFs-masonry-concrete infilled frame	91.40	87.30
(6)	3B6S MRFs-masonry-concrete infilled frame without ground infills	91.80	137.5
(7)	3B9S MRFs-bare frame	190.9	435.0
(8)	3B9S MRFs-bare frame with structural deficiencies	190.9	285.0
(9)	3B9S MRFs-stone-concrete infilled frame	126.6	216.6
(10)	3B9S MRFs-stone-concrete infilled frame without ground infills	126.7	244.9
(11)	3B9S MRFs-masonry-concrete infilled frame	127.2	212.5
(12)	3B9S MRFs-mMasonry-concrete Infilled Frame without Ground infills	127.5	240.6

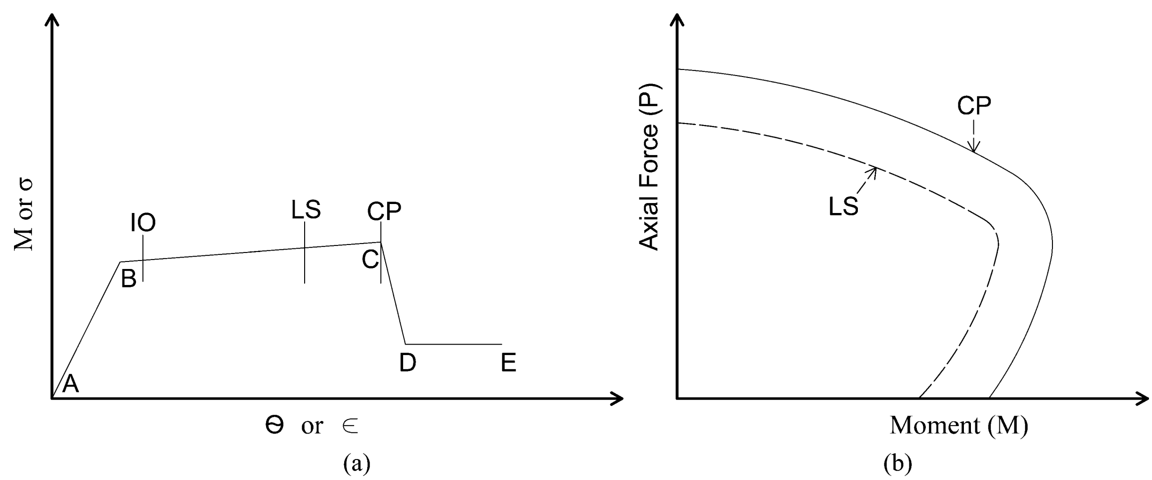

Fig. 14 **a** Force–deformation relationship for the beam, beam–column joint, and infill model. **b** Force–deformation relationship for the column

in ductility, which indicates that the R factor is lower than the design value. This implies the improper calculation of seismic forces using conventional design procedures and inadequate performance.

5.3 Performance points and element performance levels

It was difficult for some of the frames examined to identify R factors; therefore, the performance of the frames was determined and compared with the performance required by conventional design standards. The performance of each prototype frame model was evaluated for a seismic event with a probability of exceeding 10% in 50 years. According to SEI/ASCE-41 [40], life safety is the anticipated performance level. The target displacement is calculated based on the selected seismic event. The life safety objective limit is 0.75 times the maximum displacement in the pushover curve for each prototype model. Table 6 shows the target and limit displacement at the life safety performance level. A force–deformation relationship is defined for each frame element by modeling and assigning nonlinear hinges to reflect the nonlinear behavior. In the case of the beam and beam-column joint elements, a moment-rotation relationship was chosen to identify the performance of the beam and beam-column joint elements, as shown in Fig. 14a. The x-axis is set to be the rotation (Θ), and the y-axis is the moment (M). Infill models were constructed by the axial stress–strain relationship, as shown in Fig. 14a. The x-axis is set to be the strain (mm/mm), and the y-axis is the axial stress.

Furthermore, the design interaction diagram (P-M) was utilized to evaluate the seismic performance of columns at the hinges near the supports, as shown in Fig. 14b. The x-axis is set to be the moment (M), and the y-axis is the axial force (P). It was also considered that the collapse prevention performance level is located on the P—M interaction curve, and the life safety performance level is set to 0.75 times at any value lying on the P—M interaction curve [40]. At the element level, the element model's target performance (θ, ε, or M) is depicted at the time step where the target displacement is achieved. The limits for different performance objectives for each force–deformation relationship are determined following SEI/ASCE-41 [40]. The yielding point is at point B in Fig. 14a, and intermediate occupancy (IO) occurs where the deformation equals 0.67 times the deformation limit for life safety (LS). Life safety (LS) is estimated to be 0.75 times the deformation at point C. Last, collapse prevention (CP) is 1.0 times the deformation at point C on the curve.

6 Performance-based seismic assessment

6.1 3B6S MRFs: ductile and nonductile bare frame

The analysis was performed on 3B6S MRFs with ductile and nonductile (with structural deficiencies) bare frames, and the results are summarized in Fig. 15. The performance of both models at the target displacement step is within the life safety objective; in other words, none of the hinges exceeded the life safety (LS) performance level, as shown in Fig. 16. For the 3B6S MRF-ductile bare frame, the hinges in the beams and beam-column joints are distributed on all floors and reach an intermediate occupancy IO performance level. Column hinges are formed at lower levels and within the LS performance level. This indicates a swaying mechanism that is favorable for seismic activity. For the 3B6S MRF-nonductile bare frame, more hinges in columns, beams, and beam-column joints reached the LS performance level, indicating that more damage occurred to structural elements in critical positions than in the 3B6S MRF-ductile bare frame.

Furthermore, the margin between the target displacement and ultimate displacement is much smaller in the case of nonductile frames. As uncertainties are expected in terms of material properties and design parameters, this small margin imposes reliability issues for the performance and meeting its objective.

6.2 3B6S MRF-ductile bare frame, masonry-concrete infilled frame, and masonry-concrete infilled frame without ground infills

The performance and seismic behavior of the 3B6S MRFs-ductile bare frame and masonry-concrete infilled frame were compared with and without ground infills (soft story effect). The analysis results in Fig. 17 show a reduction in

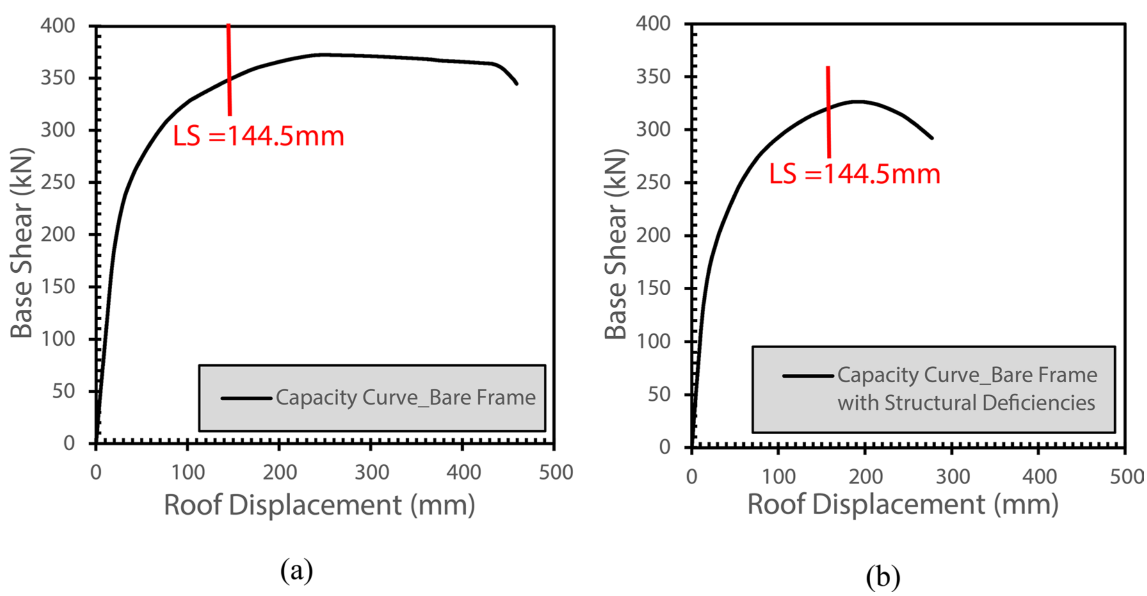

Fig. 15 Performance point and capacity curves for the 3B6S MRF (**a**) ductile bare frame; **b** nonductile bare frame

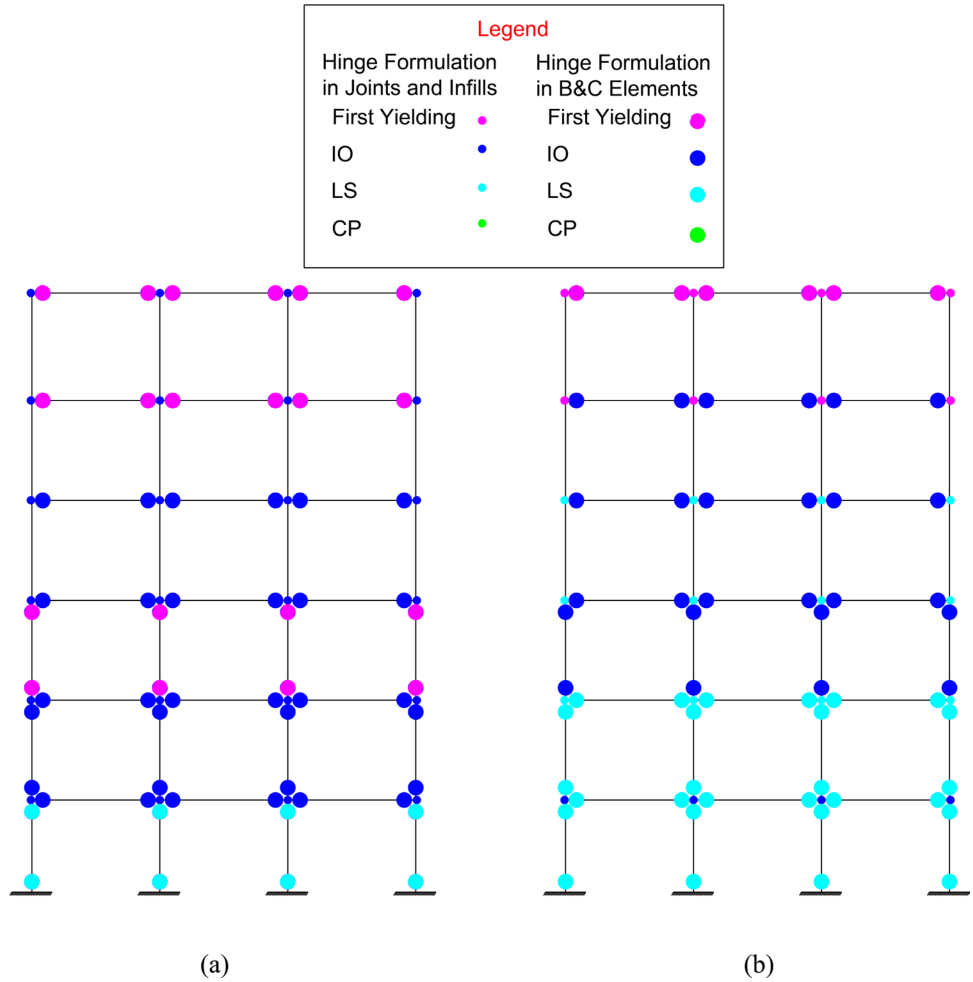

Fig. 16 Hinge formation at the assigned elements in the 3B6S MRFs (**a**) ductile bare frame; **b** nonductile bare frame

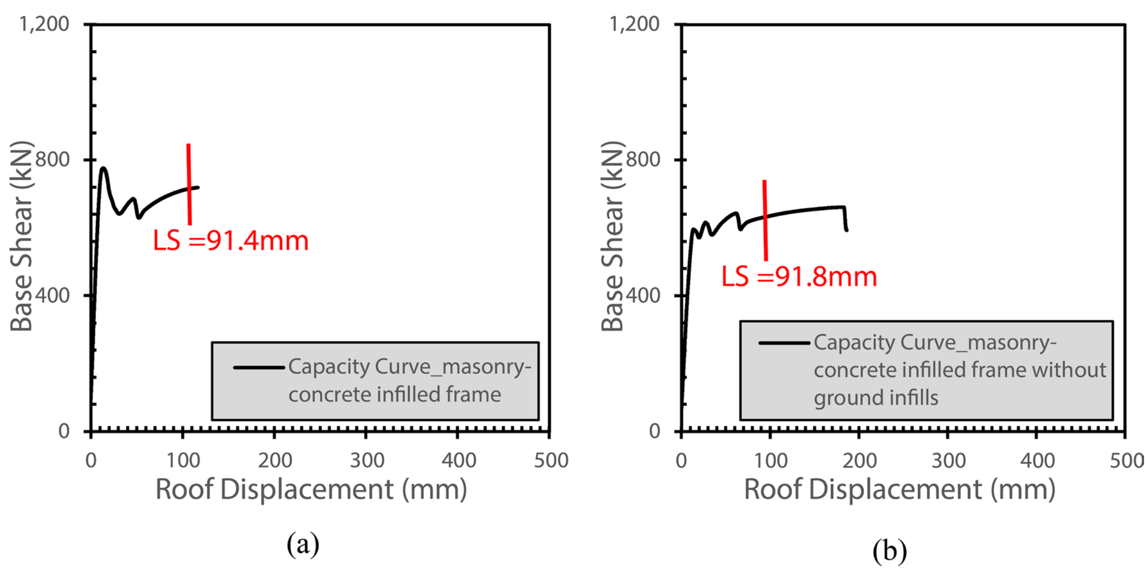

Fig. 17 Performance point and capacity curves for the 3B6S MRF (**a**) masonry-concrete infilled frame; **b** masonry-concrete infilled frame without ground infills

performance for both masonry-concrete infilled frames with and without ground infills compared with the ductile bare frame. The ultimate capacity of masonry-infilled frames is slightly greater than that of infilled frames with a soft story. In the case of the masonry–concrete infilled frame, the performance at the target displacement step is within the life safety objective, as shown in Fig. 17a. In contrast, the masonry–concrete infilled frame with a soft story reached the target displacement, with elements reaching the collapse prevention performance level, as shown in Fig. 17b. The infilled frames with a soft story did not satisfy the performance objective of conventional standards. Examining each frame's hinge type and distribution, the infilled frame has hinges distributed in the beams, beam-column joints, infills, and columns of the lower and middle floors. These are within the life safety (LS) performance level, Fig. 18a; however, their distribution pattern indicates less favorable behavior. For an infilled frame with a soft story, hinges also appear to be concentrated within the lower to middle floors. However, the joints in the ground floor columns reached the collapse prevention performance level, as shown in Fig. 18b**,** indicating soft-story mechanisms, which may lead to catastrophic failure. Furthermore, the capacity curves for both infilled frames indicate local failures and multiple sudden degradations in the capacity curve, which is not observed for the capacity curves of the ductile bare frames.

6.3 3B9S MRFs: ductile and nonductile bare frame

Similar to the behavior of 3B6S MRFs, ductile and nonductile (with structural deficiencies) bare frames were compared during the analysis of 3B9S MRFs. The 3B9S MRF ductile frame reached the target displacement step. None of the developed hinges in the beams and joints reached the life safety (LS) performance level; only the hinges on the ground floor columns reached life safety performance, Figs. 19 and 20. The developed hinges in the 3B9S MRF-nonductile bare frame have a similar pattern as those in the 3B6S MRF-ductile frame; however, more column hinges at higher floors reach life safety performance levels. Comparing both models with the performance of 3B6S MRFs- ductile and nonductile bare

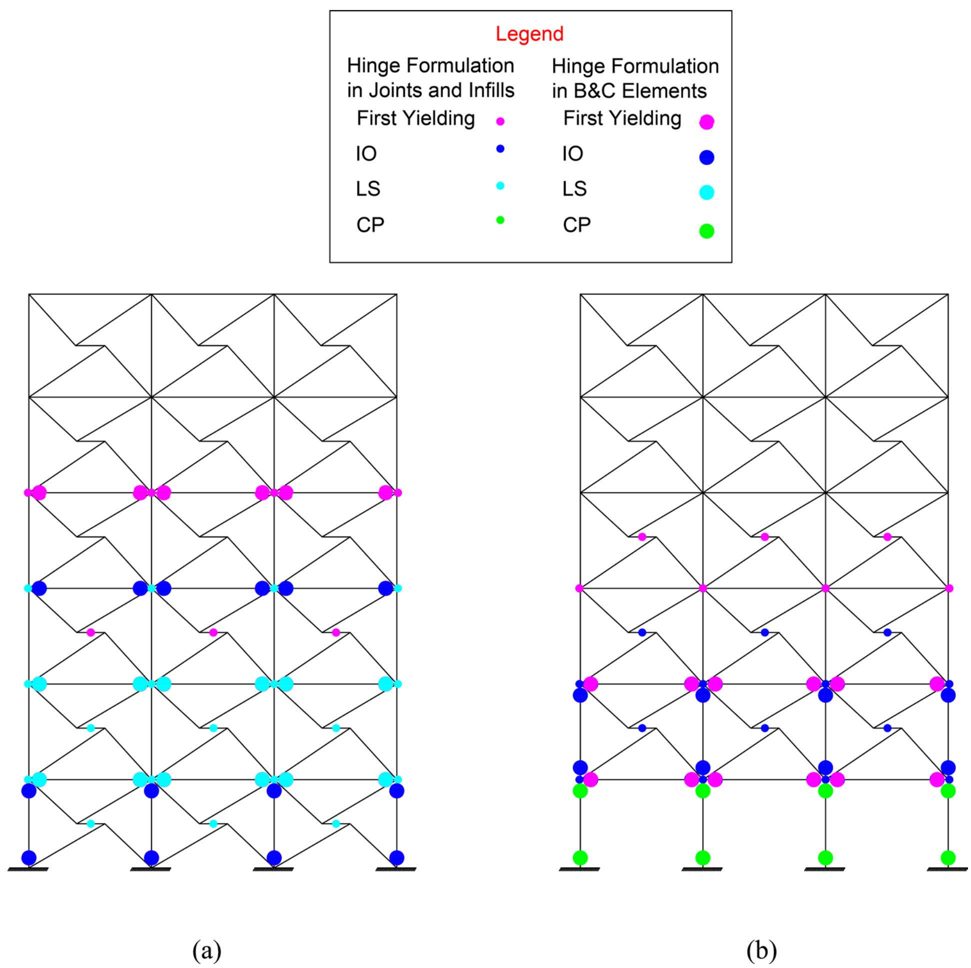

Fig. 18 Hinge formation at the assigned elements in the 3B6S MRFs (**a**) masonry concrete infilled frame; **b** masonry concrete infilled frame without ground infills

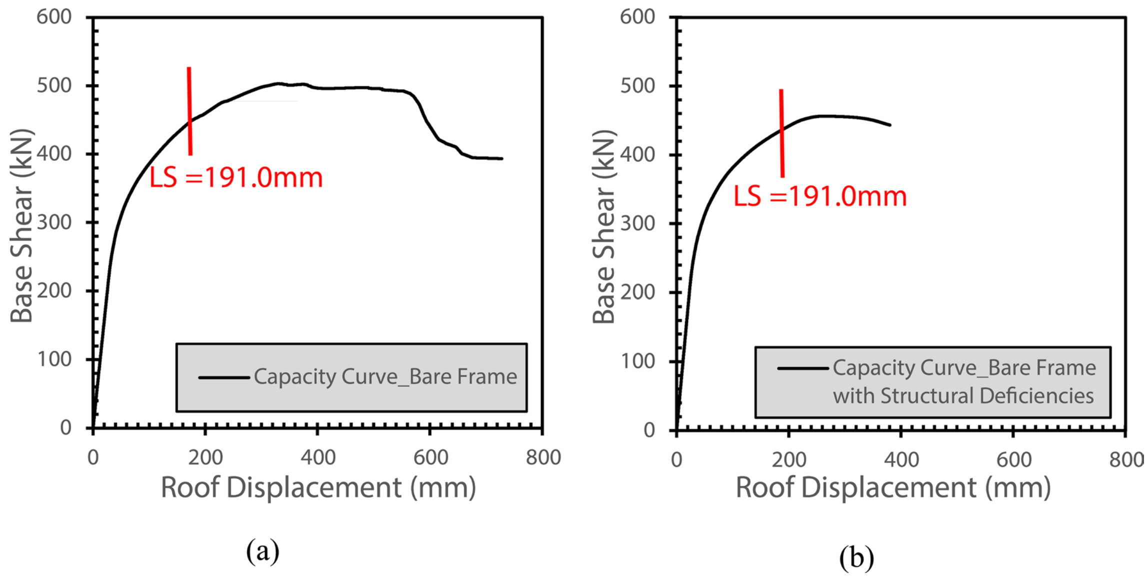

Fig. 19 Performance point and capacity curves for the 3B9S MRF (**a**) ductile bare frame; **b** nonductile bare frame

frames, it can be seen that columns in frames with higher elevations tend to form more plastic hinges at the upper floors, indicating lower performance.

6.4 3B9S MRF-ductile bare frame, masonry-concrete infilled frame, and masonry-concrete infilled frame without ground infills

Figure 21 summarizes the results of the performance level analysis of the 3B9S MRF-masonry-concrete infilled frame with and without ground infills (soft story effect). Compared with a ductile bare frame, a considerable performance loss occurs due to the existence of infills. The ultimate capacity of the infilled frames is significantly greater than that of the infilled frames with a soft ground story. The performance of the 3B9S MRF-masonry-concrete infilled frames at the target displacement step did not exceed the life safety objective, as shown in Fig. 21. Figure 22 shows that the 3B9S MRF-masonry-concrete infilled frame formed plastic hinges in the beams, columns, and infills at the LS level. The beam-column joint hinges reached the yielding point. Most hinges were concentrated at the lower and middle floor levels. In contrast, 3B9S MRFs—masonry–concrete infilled frames with soft stories—formed hinges with IO performance levels in beams and beam—column joint elements. The column hinges at the first story reached a collapse prevention performance level exceeding the LS performance level. This indicates that the activation of the soft-story mechanism and that the frame does not satisfy the performance requirements of conventional standards. A comparison is run for the 3B9S MRF-masonry-concrete infilled frame with the 3B6S MRF-masonry-concrete infilled frame, which shows that as the elevation of the frame system increases, the effect of the soft story becomes more evident.

6.5 3B6S and 3B9S MRFs-stone-concrete infilled frame with/without ground infills

The performance and behavior of the 3B6S and 3B9S MRF-stone-concrete infilled frames with/without ground infills were observed to be the same as those of the 3B6S and 3B9S MRF-masonry-concrete infilled frames with/without ground infills.

Based on the results from the nonlinear analysis, it is evident that using a response modification factor R of 8 is not appropriate, even when reinforced concrete frames are designed as special moment-resisting frames (SMRF) [1], as local practices are not accounted for. The findings suggest that a more suitable R value for such frames would range from 4 to 6, depending on the specific structural configuration, particularly in the absence of a soft story. This recommendation stems from the significant loss of ductility observed in frames with deficiencies caused by the current construction practices and the presence of infill walls (both internal and external), which hindered the expected inelastic energy dissipation. These results emphasize the need for revisions in local construction practices and their quality, alongside urgent outreach and training within the current construction industry. Additionally, seismic design parameters from international standards require further investigation and adaptation to ensure accurate and reliable seismic performance in local contexts.

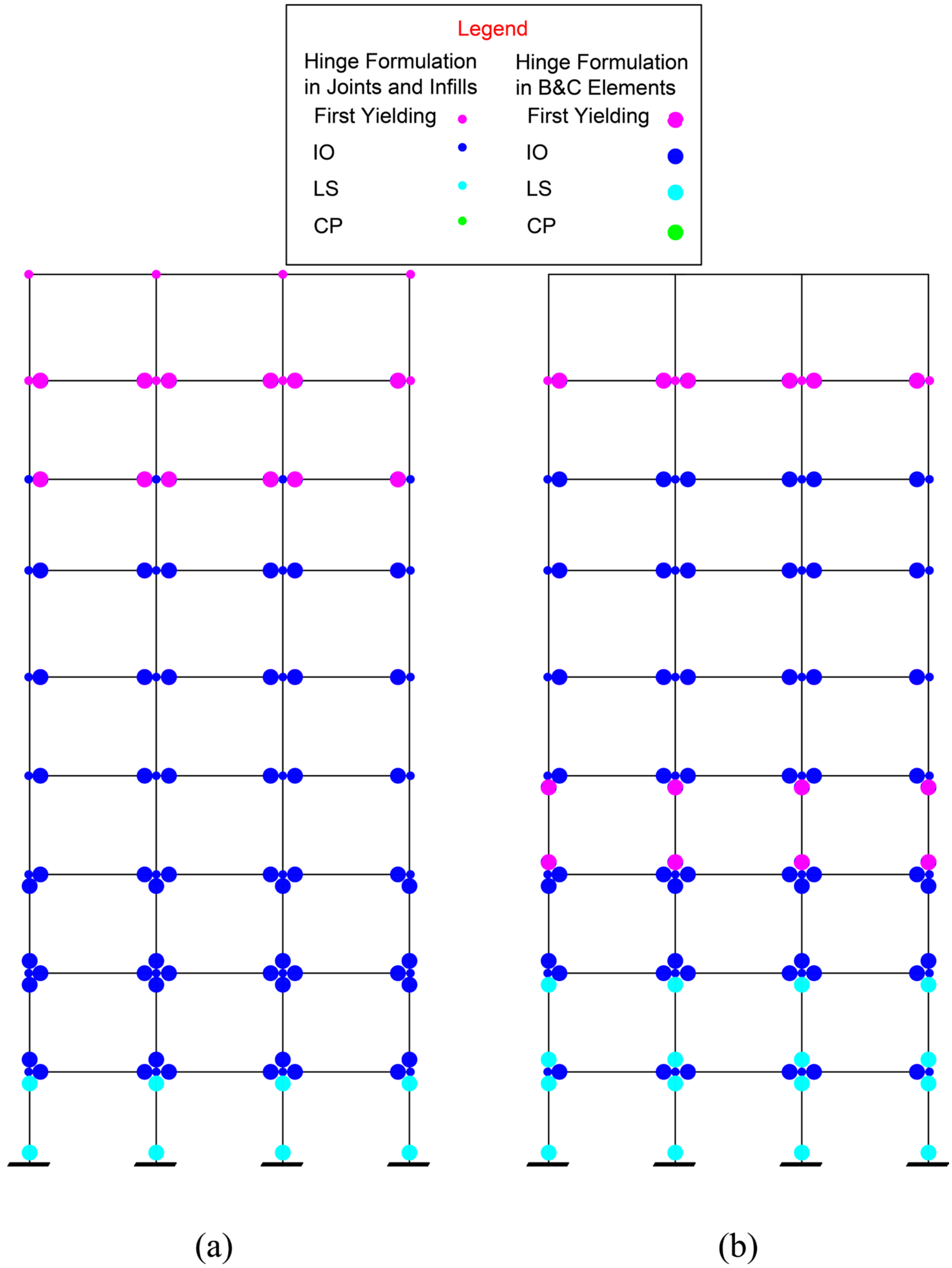

Fig. 20 Hinge formation at the assigned elements in the 3B9S MRFs (**a**) ductile bare frame; **b** nonductile bare frame

7 Conclusions

This paper analytically examined the seismic performance of deficient reinforced concrete moment resisting frames (MRFs) in Ramallah city. Numerical models of the studied structural systems were developed in OpenSees to investigate the performance of the buildings using twelve 2D RC-moment resisting frames (MRFs). Each frame system is analyzed using nonlinear static pushover analysis to evaluate the ductility and response modification factors. The performance of the buildings was further examined by running performance and damage assessments to check the frames' satisfaction with the performance requirements according to conventional standards. Based on the modeling and analysis results, it was found that the ductility factors for most of the prototypes are less than those used in the design process, indicating a lower performance than that in the design process. Structural deficiencies resulted in a poor distribution of plastic hinges in the structural elements. Consequently, a significant loss in ductility of the frame system was observed, leading to poor seismic performance in the investigated frame models. The

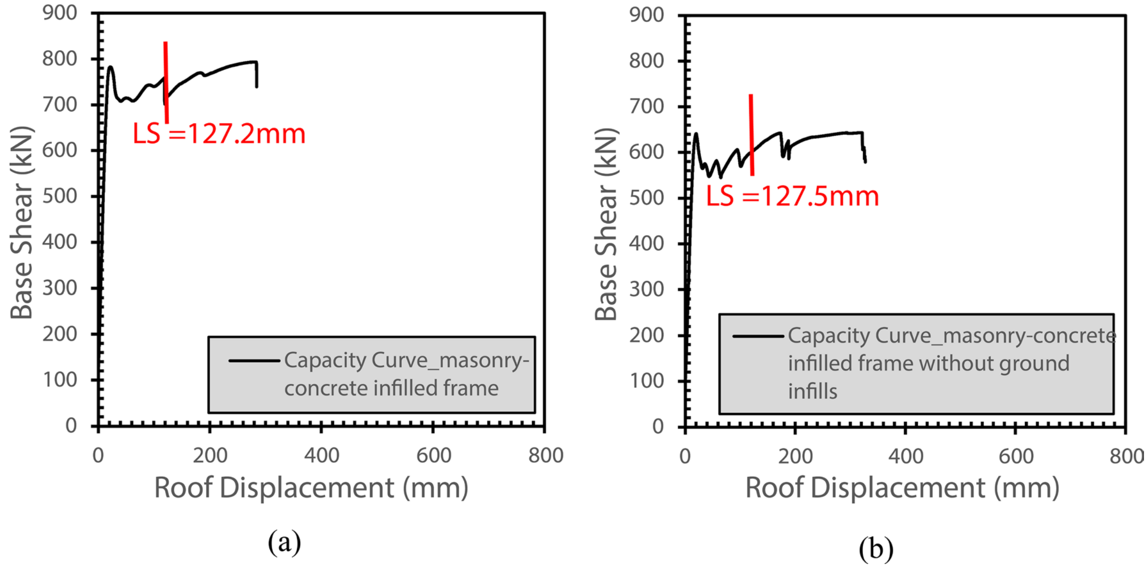

Fig. 21 Performance point and capacity curves for the 3B9S MRF (**a**) masonry-concrete infill frame performance point; **b** masonry-concrete infill frame without ground infill

building height is an important parameter affecting structural performance, especially during soft-story impact. Using stone-concrete or masonry-concrete infills dramatically decreased ductility, resulting in severe damage to some elements. Furthermore, using stone-concrete or masonry-concrete infills in frame systems without ground infills creates a soft story mechanism. Infilled frames with a soft story do not satisfy the performance requirements of conventional seismic design standards. Moreover, the study findings highlight the significant impact of labor skills, supervision, and construction techniques on the effectiveness of the design and the achievement of anticipated behavior and performance. Pushover analysis and lumped plasticity models with predefined plastic hinges were used to represent the nonlinear behavior of the frame elements. Although these methods are widely accepted for seismic evaluation, they have certain limitations. Pushover analysis simplifies dynamic seismic responses by applying static load conditions, which may not fully capture higher mode effects or complex structural responses. Similarly, lumped plasticity models concentrate inelastic behavior at specific points, potentially overlooking distributed damage across the structural element. Furthermore, the study was based on twelve (2D) frame models representing a building configuration category. Despite these limitations, this pilot study offers valuable insights into the impact of local building technology on code compliance while highlighting the influence of non-structural components, such as cladding and internal walls, on seismic performance. The study's results will guide future work in evaluating frames under seismic events with different configurations using 3D modelling.

The following are recommendations for enhancing the behavior of buildings:

- Strict supervision related to structural detailing to preclude shortcomings, such as inadequate joint shear reinforcement, insufficient development length of beam bars, and inadequate stirrup spacing in beams and columns.
- A more in-depth analysis of new buildings designed for seismic action with a response modification factor greater than 5, based on assumed ductility level according to SEI/ASCE7 [1].
- Construction detail development for separation between the infill and the frame system developed based on local construction practice. This approach could be applied using anchored joints and providing a seismic gap between the infills and the frame system.
- The relative ductility of infill walls can be increased by using reinforced masonry.
- Alternatives to the stone cladding of reinforced concrete buildings include, e.g., foam stone with less weight and lower rigidity.
- More training was provided for practicing engineers and construction workers on the critical role of proper detailing in seismic resistance, ensuring the understanding of the impact of inadequate construction practices.
- Workshops on constructing partitions and properly implementing separation joints, emphasizing their importance for maintaining structural integrity during earthquakes.

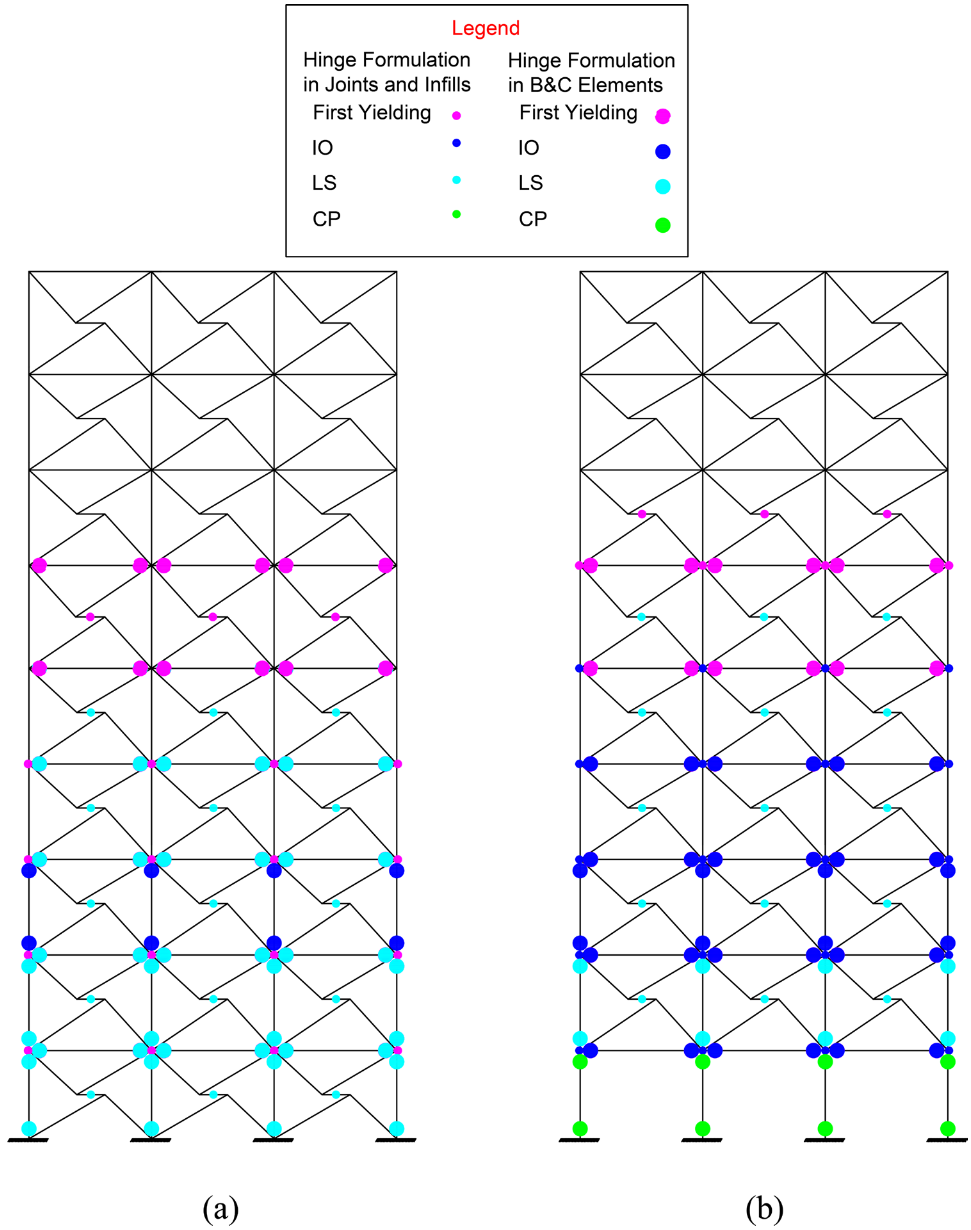

Fig. 22 Hinge formation at the assigned elements in the 3B9S MRFs (**a**) masonry concrete infilled frame; **b** masonry concrete infilled frame without ground infills

Author contributions M. S. Conceptualizing, methodology, data collection and analysis, investigation, writing-original draft. G. K. Conceptualizing, methodology, supervision, investigation, writing—reviewing and editing.

This manuscript is based on the author's master's thesis, 'Seismic performance of deficient reinforced concrete frames in developing countries: A case study in Ramallah City,' submitted to Birzeit University, West Bank, Palestine in 2022.

Funding The authors declare that no funds, grants, or other support was received during the preparation of this manuscript.

Data availability Some of the data, models, or codes that support the findings of the current study are available from the corresponding author upon reasonable request.

Declarations

Competing interests The authors declare no competing interests.

References

1. SEI/ASCE7. Minimum Design Loads and Associated Criteria for Buildings and Other Structures (Minimum Design Loads and Associated Criteria for Buildings and Other Structures). 2016.
2. ACI-318-14: Building Code Requirements for Structural Concrete and Commentary. ACI-318, 2014.
3. Wu J. Inelastic response spectra with high damping. J Struct Div ASCE. 1989;115(6):1412–31.
4. Hanson RD, Aiken ID, Nims DK, Richter P, Bachman R. State-of-the-art and state-of-the-practice in seismic energy dissipation. Proc Semin Seismic Isolat Passive Energy Dissipat Active Contr Appl Technol Council. 1993;2:449–71.
5. Newmark NM, Hall WJ. Earthquake spectra and design. Engineering monographs on earthquake criteria. 1982.
6. UBC. International building code. International Code Council, USA, 1997.
7. FEMA. NEHRP guidelines for the seismic rehabilitation of buildings. Federal Emergency Management Agency, 1997.
8. NEHRP. NEHRP recommended provisions (National Earthquake Hazards Reduction Program) for seismic regulations for new buildings and other structures. Building Seismic Safety Council, 2001.
9. Zafar A. Response modification factor of reinforced concrete moment resisting frames in developing countries. Master of Science in Civil Engineering Master Thesis, Department of Civil Engineering (M.Sc Thesis), University of Illinois at Urbana-Champaign, Illinois, 2009.
10. Mondal A, Ghosh S, Reddy G. Performance-based evaluation of the response reduction factor for ductile RC frames. Eng Struct. 2013;56:1808–19.
11. Chaulagain H, Rodrigues H, Spacone E, Guragain R, Mallik R, Varum H. Response reduction factor of irregular RC buildings in Kathmandu valley. Earthq Eng Eng Vib. 2014;13:455–70.
12. Indian Standard I. Criteria for earthquake resistant design of structures. Bureau of Indian Standards, New Delhi, pp. 1–24, 2002.
13. Kim J, Choi H. Response modification factors of chevron-braced frames. Eng Struct. 2005;27(2):285–300.
14. Badrashi E, Irfan Y. Response modification factors for reinforced concrete buildings in Pakistan. University of Engineering & Technology Peshawar. 2016.
15. Akbar J, Ahmad N, Alam B. Response modification factor of haunch retrofitted reinforced concrete frames. J Perform Constr Facil. 2020;34(6):04020115.
16. Cui S, Chen Y, Lu D. Probability assessment of structural response modification factor of RC frames by the demand-capacity-factor method. Structures. 2021;30:628–37.
17. Abuznaid H. Response modification factor in intermediate moment resisting frame building. 2023.
18. Caballero-Castro LF, Cano-Castaño HA, Molina-Herrera M, Villalba-Morales JD, Arroyo O. Evaluating the response modification factor (R) for reinforced concrete and steel structures equipped with TADAS devices designed for high seismic hazard in Colombia. Structures. 2024;65:106748.
19. Pampanin S, Calvi GM, Moratti M. Seismic behavior of RC beam-column joints designed for gravity only. 2002.
20. Park R. A summary of results of simulated seismic load tests on reinforced concrete beam-column joints, beams and columns with substandard reinforcing details. J Earthquake Eng. 2002;6(02):147–74.
21. Shafaei J, Zareian MS, Hosseini A, Marefat MS. Effects of joint flexibility on lateral response of reinforced concrete frames. Eng Struct. 2014;81:412–31.
22. Rajeev A, Parsi SS, Raman SN, Ngo T, Shelke A. Experimental and numerical investigation of an exterior reinforced concrete beam-column joint subjected to shock loading. Int J Impact Eng. 2020;137: 103473.
23. Lin WW-C. Modelling effects of insufficient lap splices on a deficient reinforced concrete frame. Middle East Technical University, 2013.
24. Kumbasaroglu A. Effect of anchor bars on seismic behavior of infilled walled frames. KSCE J Civ Eng. 2020;24(10):2980–92.
25. Pandit T, Chaulagain H. Evaluation of response reduction factor of existing masonry infilled RC-buildings in Pokhara. Himalayan J Appl Sci Eng. 2020;1(1):41–51.
26. Patel N, Vasanwala SA. Evaluation of response reduction factor for un-reinforced masonry-infilled RC buildings. In: Innovations in Infrastructure: Proceedings of ICIIF 2018, 2019: Springer, pp. 525–535.
27. Ko H, Park Y-K, Lee D-G. Evaluation of seismic behavior for low-rise RC moment resisting frame with masonry infill walls. In: 14th World Conference on Earthquake Engineering (14WCEE), Beijing, China, 2008.
28. Kumbasaroğlu A, Budak A. An experimental study on impact of anchor bars at the steel frames with infilled walls. Challenge. 2016;2(2):129–38.
29. Al-Tarazi EA. Regional seismic hazard study for the eastern Mediterranean (Trans-Jordan, Levant and Antakia) and Sinai region. J Afr Earth Sci. 1999;28(3):743–50.
30. Shapira A. Magnitude scales for regional earthquakes monitored in Israel. Israel J Earth-Sci. 1988;37(1):17–22.
31. Abou Karaki N. Synthèse et carte sismotectonique des pays de la bordure orientale de la Méditerranée: sismicité du système de failles du Jourdain-Mer Morte. Université Louis Pasteur (Strasbourg) (1971–2008), 1987.
32. Al-Dabbeek JN, El-Kelani RJ. Rapid assessment of seismic vulnerability in Palestinian refugee camps. J Appl Sci. 2008;8(8):1371–82.
33. Al-Dabbeek JN. Vulnerability, and expected seismic performance of buildings in West Bank, Palestine. Islamic Univ J. 2007;15(1):193–217.

34. Salahat FH. Seismic performance-based assessment and retrofit of a typical reinforced concrete building in Palestine. University of Birmingham, 2014.
35. Al-Taie E, Al-Ansari N, Knutsson S. The need to develop a building code for Iraq. Engineering. 2014;6(10):610–32.
36. Shkoukani HT. General rules for design of reinforced concrete structures according to Eurocode No. 2: Comparative with the ACI Code. 1993.
37. Grigoratos I, et al. Development of a fragility and exposure model for Palestine—application to the city of Nablus. Proc Eng. 2016;161:2023–9.
38. Al-Nimry H, Resheidat M, Qeran S. Rapid assessment for seismic vulnerability of low and medium rise infilled RC frame buildings. Earthq Eng Eng Vib. 2015;14:275–93.
39. Structural response modification factors, ATC, Applied Technology Council, Redwood City, California, 1995.
40. SEI/ASCE-41. Seismic evaluation and retrofit of existing buildings. 2017: American Society of Civil Engineers.
41. Freeman S. On the correlation of code forces to earthquake demands. In: Proceedings of 4th US–Japan workshop on improvement of building structural design and construction practices, ATC-15-3 report. Redwood City, California, 1990.
42. Mazzoni S, McKenna F, Scott MH, Fenves GL. OpenSees command language manual. In: Pacific Earthquake Engineering Research (PEER) Center. 2006;264(1): 137–158.
43. Yassin MHM. Nonlinear analysis of prestressed concrete structures under monotonic and cyclic loads. Berkeley: University of California; 1994.
44. Mander JB, Priestley MJ, Park R. Theoretical stress-strain model for confined concrete. J Struct Eng. 1988;114(8):1804–26.
45. Lowes LN, Altoontash A. Modeling reinforced-concrete beam-column joints subjected to cyclic loading. J Struct Eng. 2003;129(12):1686–97.
46. Viwathanatepa S, Popov EP, Bertero VV. Effects of generalized loadings on bond of reinforcing bars embedded in confined concrete blocks. University of California, Earthquake Engineering Research Center Oakland, CA, 1979.
47. Anderson M, Lehman D, Stanton J. A cyclic shear stress–strain model for joints without transverse reinforcement. Eng Struct. 2008;30(4):941–54.
48. Kim J, LaFave JM, Song J. Joint shear behaviour of reinforced concrete beam–column connections. Mag Concr Res. 2009;61(2):119–32.
49. Jeon J-S, Lowes LN, DesRoches R, Brilakis I. Fragility curves for non-ductile reinforced concrete frames that exhibit different component response mechanisms. Eng Struct. 2015;85:127–43.
50. Rodrigues HFP. Desenvolvimento e calibração de modelos numéricos para a análise sísmica de edifícios. 2005.
51. Mainstone RJ. Summary of paper 7360. On the stiffness and strengths of infilled frames. Proc Inst Civil Eng. 1971;49(2):230.
52. Dolšek M, Fajfar P. Mathematical modelling of an infilled RC frame structure based on the results of pseudo-dynamic tests. Earthquake Eng Struct Dynam. 2002;31(6):1215–30.
53. Žarnić R, Gostič S. Masomy infilled frames as an effective structural sub-assemblage. In: Seismic design methodologies for the next generation of codes. New York: Routledge; 2019. p. 335–46.
54. Al-Nimry. Seismic vulnerability of residential buildings in Jordan and its locality. In: Proceedings of the 15th World Conference on Earthquake Engineering, 2012.
55. Al-Nimry H. Evaluation of seismic performance of stone-concrete residential buildings in Jordan. Final Report. 2010.
56. Al-Nimry HS. Quasi-static testing of RC infilled frames and confined stone-concrete bearing walls. J Earthquake Eng. 2014;18(1):1–23.
57. Fajfar P, Dolsek M, Zarnic R, Gostic S. Development of numerical methodologies for infilled frames, towards European integration in seismic design and upgrading of building structures project. Euroquake-project, Final report. 2001.
58. Vecchio FJ, Emara MB. Shear deformations in reinforced concrete frames. ACI Struct J. 1992;89(1):46–56.
59. Cavaleri L, Fossetti M, Papia M. Effect of vertical loads on lateral response of infilled frames. In: Proceedings 13th World Conference on Earthquake Engineering. 2004.